Climate Variability Induced by Anomalous Buoyancy Forcing in a Multilayer Model of the Ventilated Thermocline*

Rui Xin Huang and Joseph Pedlosky

Department of Physical Oceanography, Woods Hole Oceanographic Institution, Woods Hole, Massachusetts

ABSTRACT

Climate variability induced by surface cooling in a four-moving-layer model of the ventilated thermocline is studied. The perturbations propagate within the characteristic cones defined by streamlines in individual layers where the potential vorticity anomaly is created. Each time the characteristic cones cross a new outcrop line, the number of characteristic cones doubles. Thus, climate variability in a multilayer model can have very complicated structure in the horizontal plane, with anomalies of alternating sign. The vertical structure of such perturbations defines a class of dynamical thermocline modes.

1. Introduction

Climate variability on decadal timescales can be examined by perturbing the steady solution of the thermocline in a multilayer model. Huang and Pedlosky (1999) studied a simple two-layer model for the ventilated thermocline and revealed the horizontal and vertical structure of the perturbations. In response to a surface cooling anomaly, the perturbations are horizontally confined to a characteristic cone defined by the streamlines stemming from the western and eastern edges of the cooling source.

The vertical structure of the response to the cooling anomaly depends on the structure of the thermocline circulation in which it is embedded. Therefore, we term such structures "dynamical thermocline modes" and they are distinct from, though reminiscent of, the standard geostrophic vertical normal modes of a resting ocean.

An attempt was made by Huang and Pedlosky (1999) to explore the structure of the perturbations for a model with three moving layers. The addition of one more moving layer makes the dynamics much more complicated because a new characteristic cone is created when the primary characteristic cone crosses a new outcrop line. A careful examination reveals that the structure of the perturbations due to a surface forcing anomaly in a

multilayer model can be extremely complicated when the number of moving layers increases. In fact, we are chagrined to note that some part of the discussion about the case of three-moving layers presented by Huang and Pedlosky (1999) is in error.

In particular, we will show that the anomalies produced by a localized cooling excite a fan of characteristics that broadens as the perturbations move southward. The disturbance produces a chain reaction of potential vorticity anomalies that because of the beta spiral, constantly expand the zone of influence of a single disturbance. In this paper we will examine the climate variability for a model with three and four moving layers. It is this cascade, or chain reaction, that we overlooked in our previous paper.

2. Model formulation

In this paper, we will use a notation slightly different from that used in the classic ventilated thermocline model of Luyten et al. (1983). We denote the bottom and motionless layer as layer 0 and the lowest moving layer as layer 1, and the layers above have number increases upward, Fig. 1. The thickness and the depth of the ith layer are denoted as h_i and H_i, respectively; thus, for the top layer n, $H_n = h_n$. The northernmost outcrop line is labeled as f_1, and the outcrop lines southward have number indices that increase accordingly. This notation is more convenient when one has to deal with an arbitrary number of layers.

a. Pressure gradient in multilayer model

First we derive a relation between pressure gradients in two adjacent layers. Using the hydrostatic relation, the pressure gradient in two adjacent layers satisfies

Corresponding author address: Rui Xin Huang, Department of Physical Oceanography, Wood Hole Oceanographic Institution, Woods Hole, MA 02543.
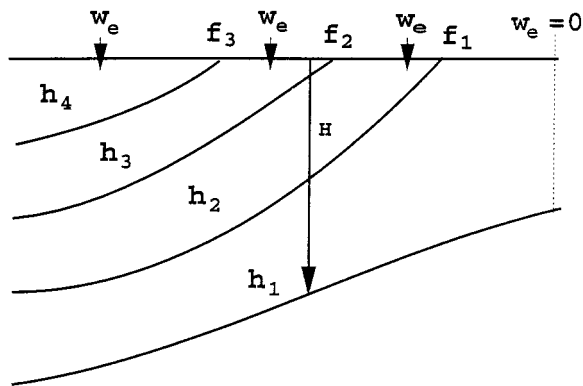E-mail: rhuang@whoi.edu

FIG. 1. A sketch of the multilayer model.

$$\frac{\nabla P_i}{\rho_i} = \frac{\nabla P_{i-1}}{\rho_i} + \gamma_i \nabla H_i, \qquad (1)$$

where

$$\gamma_i = g\frac{\rho_{i-1} - \rho_i}{\rho_i}$$

is the reduced gravity across the interface. This relation applies to any pair of layers. In addition, one can assume that the lowest layer with subscript 0 is very deep, so that the pressure gradient there is negligible. Thus, the pressure gradient in the mth layer ($m \leq n$) is

$$\frac{\nabla P_m}{\rho_0} = \sum_{i=1}^{m} \gamma_i H_i. \qquad (2)$$

b. The Sverdrup relation

By taking the curl of the momentum equations in each layer the vorticity balance is obtained. Multiplying by the layer depth, summing up over all the moving layers, and integrating over $[x, x_e]$, one obtains the Sverdrup relation

$$\sum_{i=1}^{n} \gamma_{i1} H_i^2 = D_0^2 + H_0^2, \qquad (3)$$

where

$$D_0^2 = -\frac{2f}{\beta\gamma_1} \int_x^{x_e} w_e(x', y)\, dx'; \qquad \gamma_{i1} = \frac{\gamma_i}{\gamma_1}$$

$$H_0^2 = \sum_{i=1}^{n} \gamma_{i1} H_{ie}^2. \qquad (4)$$

Perturbing the Sverdrup relation gives, to the lowest order,

$$\sum_{i=1}^{n} \gamma_{i1} H_i \delta H_i = \frac{1}{2}\delta D_0^2. \qquad (5)$$

Since anomalous buoyancy forcing makes no contribution to the right-hand side of (5), climate variability due to surface temperature (or freshwater flux) pertur-

bations must appear as an internal mode, with a depth-weighted zero mean. We call such modes, which satisfy the homogeneous form of (5), *dynamical thermocline modes* (DTM hereafter) since the modal structure will be a function of the background thermocline structure that varies laterally. On the other hand, anomalous wind stress forcing can lead to the first baroclinic DTM.

c. Region II

We start our discussion by describing the anomalies produced in layer 1 and 2 in the region $f_2 < f < f_1$, denoted as region II in Fig. 2. South of the first outcrop line y_1, potential vorticity in layer 1 is conserved along the streamline, $h_1 = H_1 = $ const:

$$Q_1(H_1) = \frac{f}{h_1} = \text{const.} \qquad (6)$$

At $f = f_1$, $h_1 = H_1$; thus, the functional form of Q_1 is $Q_1(x) = f_1/x$, and the first layer thickness is

$$h_1 = \frac{f}{f_1}H_1. \qquad (7)$$

The solution in region II is

$$H_1 = \left(\frac{D_0^2 + H_0^2}{G_2}\right)^{1/2}, \qquad (8)$$

where

$$G_2 = 1 + \gamma_{21}\left(1 - \frac{f}{f_1}\right)^2. \qquad (9)$$

We introduce the fractional layer thicknesses, F, which is defined as the layer thickness divided by the total depth of the ventilated layers; thus, for region II we have

$$F_1^{II} = \frac{h_1}{H_1} = \frac{f}{f_1}, \qquad (10)$$

$$F_2^{II} = \frac{h_2}{H_1} = 1 - \frac{f}{f_1}, \qquad (11)$$

where the superscript II indicates that the definition applies to region II with two moving layers, and the subscripts indicate the individual layers.

It is important to note that f_1 in these relations is not necessarily a constant. In fact, we can write it in the form of $f_1(H_1)$, which indicates that f_1 is dependent on the latitude of the outcrop line by tracing backward along the streamline $H_1 = $ const. Therefore, in our discussion hereafter, we can write alternatively $f_1 \Rightarrow f_1 + \delta f_1$, where we imagine that δf_1 represents the outcrop line perturbations induced by heating or cooling anomaly. If $\delta f_1 < 0$, this implies that outcrop line moves equatorward from its constant value of f_1 representing cooling.
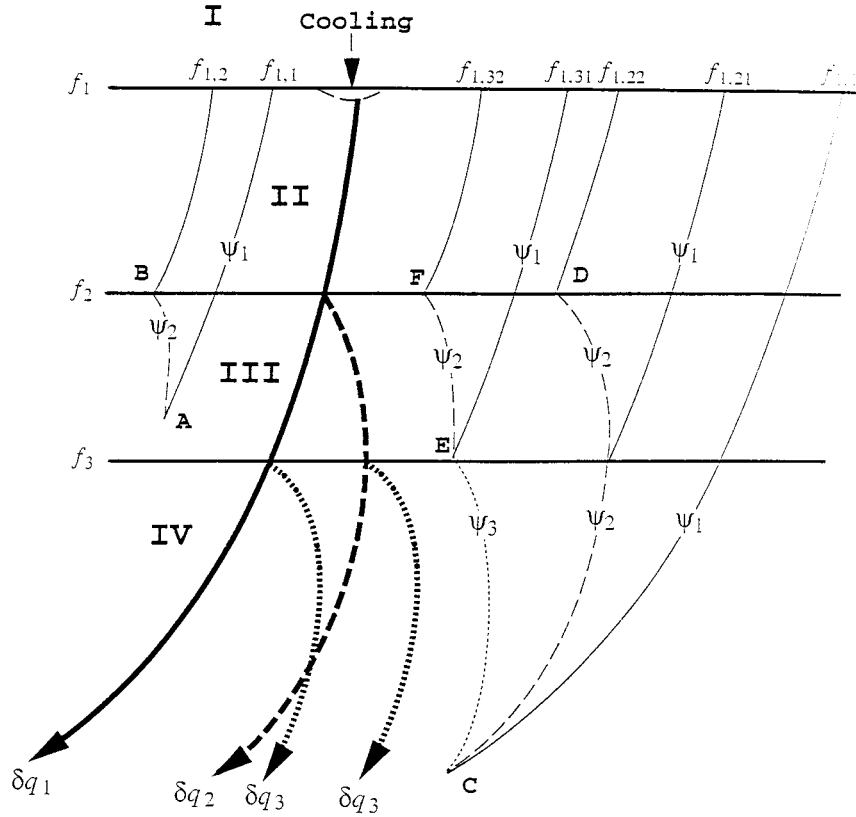
Since along the first outcrop line

FIG. 2. Potential vorticity anomalies and streamlines tracing the original outcrop lines.

$$H_1^2 = -\frac{2f_1^2(x)}{\beta\gamma_1} \int_x^{x_e} w_e(x', y)\, dx' + H_e^2, \quad (12)$$

it is readily shown that

$$H_1^2(x) = H_{10}^2(x) + O(\delta f_1),$$

where $H_{10}(x)$ is the total layer thickness along the unperturbed outcrop line. Thus, to the lowest-order approximation, the functional relation between H_1 and x remains unchanged. Using this relation we can calculate x and $\delta f_1(x)$ for given H_1 in order to complete the necessary inversion to determine $f_1(H_1)$ to lowest order. Accordingly, the solution in region II can be calculated either by solving the nonlinear equations (8) and (9) or using their linearized versions.

d. Climate variability induced by surface cooling

Cooling can be represented by a southward perturbation of the first outcrop line,

$$\delta f_1 < 0, \quad (13)$$

$$\delta F_1^{II} = -\frac{f}{f_1^2}\delta f_1 > 0, \quad (14)$$

$$\delta F_2^{II} = -\delta F_1^{II} < 0, \quad (15)$$

$$\delta G_2 = 2\gamma_{21}(1 - F_1^{II})\frac{f}{f_1^2}\delta f_1 < 0. \quad (16)$$

Therefore, the cooling-induced changes in the layer depth are

$$\delta H_1 = -\frac{H_1}{2G_2}\delta G_2 > 0, \quad (17)$$

$$\delta h_1 = F_1^{II}\delta H_1 + H_1\delta F_1^{II}$$

$$= \frac{H_1}{G_2}[1 + \gamma_{21}(1 - F_1^{II})]\delta F_1^{II} > 0, \quad (18)$$

$$\delta h_2 = \delta H_1 - \delta h_1 = -\frac{H_1}{G_2}\delta F_1^{II} < 0. \quad (19)$$

These results are exactly the same as the two-moving-layer case discussed by Huang and Pedlosky (1999).

e. Region III

South of f_2 there are two subsurface layers in which the streamlines are $H_1 = \text{const}$ and $H_1 + \gamma_{21}H_2 = \text{const}$. Along these streamlines potential vorticity is conserved. Note that, when the potential vorticity anomaly carried by the streamlines in layer 1 (labeled as δq_1 in Fig. 2) crosses the second outcrop line f_2, a new characteristic is created, and south of f_2 the potential vorticity anomaly in layer 2 propagates along streamlines in layer 2, labeled as δq_2 in Fig. 2. Thus the zone influenced by

the cooling broadens in a fanlike manner as the fluid moves southward.

Similar to the discussion in the previous section, at an interior point A in region III potential vorticity anomalies in layer 1 are set up by perturbations at positions along the first outcrop line f_1 obtained by tracing back along ψ_1. We introduce the notation

$$f_{n,m} = f_n(\psi_m) \tag{20}$$

to be the position of the nth outcrop line influencing a field point by tracing upstream from the point to the outcrop line starting along a streamline of layer m. For an interior point like A in Fig. 2 the potential vorticity in layer 1 is set up by tracing backward to the first outcrop line f_1 along ψ_1 (the streamline in layer one) in both regions III and II. Thus, the potential vorticity functional form and the thickness of layer 1 are

$$Q_1(H_1) = \frac{f_{1,1}}{H_1}, \qquad h_1 = \frac{f}{f_{1,1}} H_1. \tag{21}$$

The potential vorticity in layer 2 at the same point A is, however, set up at point B, which is defined by tracing backward along ψ_2 in region III. At point B, the lowest layer thickness is

$$h_1 = \frac{f_2}{f_{1,2}} H_1, \tag{22}$$

where the subscript in $f_{1,2}$ indicates that the corresponding position on the first outcrop line f_1 is now determined by tracing ψ_2 backward in region III, and then along ψ_1 in region II. At the second outcrop line f_2, thus, we have

$$h_2 = \left(1 - \frac{f_2}{f_{1,2}}\right) H_1. \tag{23}$$

Let

$$x = H_1 + \gamma_{21} H_2. \tag{24}$$

Along f_2, we have

$$x = H_1\left[1 + \gamma_{21}\left(1 - \frac{f_2}{f_{1,2}}\right)\right]. \tag{25}$$

Therefore the functional form of potential vorticity in the second layer is

$$Q_2(x) = \frac{f_2}{h_2} = \frac{f_2}{(1 - f_2/f_{1,2})} \frac{1 + \gamma_{21}(1 - f_2/f_{1,2})}{x}. \tag{26}$$

South of f_2,

$$h_1 = \frac{f}{f_{1,1}} H_1. \tag{27}$$

Thus, from (24) we obtain

$$x = H_1\left[1 + \gamma_{21}\left(1 - \frac{f}{f_{1,1}}\right)\right]. \tag{28}$$

Substituting (28) into the relation of Q_2 leads to the fractional layer thickness in region III:

$$F_1^{III} = \frac{f}{f_{1,1}}, \tag{29}$$

$$F_2^{III} = \frac{f}{f_2}\left(1 - \frac{f_2}{f_{1,2}}\right)\frac{1 + \gamma_{21}(1 - f/f_{1,1})}{1 + \gamma_{21}(1 - f_2/f_{1,2})}, \tag{30}$$

$$F_3^{III} = 1 - F_1^{III} - F_2^{III}. \tag{31}$$

The Sverdrup relation for region III is

$$H_1 = \left(\frac{D_0^2 + H_0^2}{G_3}\right)^{1/2}, \tag{32}$$

where

$$G_3 = 1 + \gamma_{21}(1 - F_1^{III})^2 + \gamma_{31}(1 - F_1^{III} - F_2^{III})^2. \tag{33}$$

The solution in region III can be obtained by solving the nonlinear equations (29)–(33). Note that both $f_{1,1}$ and $f_{1,2}$ are complicated nonlinear functions of the local total layer depth H_1, and these functions are defined by tracing back along streamlines ψ_1 and ψ_2, as shown in the upper left part of Fig. 2. For example,

$$f_{1,2} = f_{1,2}(H_1 + \gamma_{21}H_2) = f_1(H_{1,0}) \tag{34}$$

is a nonlinear function of the local total layer depth H_1, and this function can be obtained by tracing backward along ψ_2 in region III to point B and then following ψ_1 in region II, as shown in the upper left part of Fig. 2:

$$H_1(1 + \gamma_{21}(1 - f/f_{1,1}))$$
$$= H_{1,0}(1 + \gamma_{21}(1 - f_2/f_{1,2})). \tag{35}$$

Climate variability induced by anomalous buoyancy forcing can be calculated by taking the perturbations of these equations

$$\delta F_1^{III} = -\frac{f}{f_{1,1}^2}\delta\mathbf{f}_{1,1}, \tag{36}$$

$$\delta F_2^{III} = \gamma_{21}\frac{f^2}{f_2 f_{1,1}^2}\frac{1 - f_2/f_{1,2}}{1 + \gamma_{21}(1 - f_2/f_{1,2})}\delta\mathbf{f}_{1,1}$$
$$+ \frac{f[1 + \gamma_{21}(1 - f/f_{1,1})]}{f_2 f_{1,2}^2}$$
$$\times \frac{f + \gamma_{21}(f - f_2)(1 - f_2/f_{1,2})}{[1 + \gamma_{21}(1 - f_2/f_{1,2})]^2}\delta\mathbf{f}_{1,2}. \tag{37}$$

These relations clearly indicate that *in region III climate variability induced by anomalous buoyancy forcing comes from two sources*: First, the primary potential vorticity anomaly propagating along ψ_1, as denoted by $\delta\mathbf{f}_{1,1}$; second, the second potential vorticity anomaly propagating along ψ_2, as denoted by $\delta\mathbf{f}_{1,2}$. The corresponding layer thickness perturbations are

$$\delta H_1 = -\frac{H_1}{2G_3}\delta G_3 \qquad (38)$$

$$\delta G_3 = -2[\gamma_{21}(1 - F_1^{III}) + \gamma_{31}(1 - F_1^{III} - F_2^{III})]\delta F_1^{III}$$
$$- 2\gamma_{31}(1 - F_1^{III} - F_2^{III})\delta F_2^{III} \qquad (39)$$

$$\delta h_1 = H_1\delta F_1^{III} + F_1^{III}\delta H_1, \qquad (40)$$

$$\delta h_2 = H_1\delta F_2^{III} + F_2^{III}\delta H_1, \qquad (41)$$

$$\delta h_3 = \delta H_1 - \delta h_1 - \delta h_2. \qquad (42)$$

f. Region IV

The solution in region IV is much more complicated because two new characteristics, each carrying a potential vorticity anomaly in layer 3, are created when the trajectories carrying the primary and second potential vorticity anomaly across f_3, Fig. 2. Thus, *there are four potential vorticity anomaly trajectories, including the primary, the secondary, and the tertiary potential vorticity anomaly.* The solution for this region is included in the appendix.

3. Climate variability

In this section we will primarily focus on the climate variability induced by anomalous buoyancy forcing imposed along the outcrop lines. The model basin is a rectangular basin 60° wide and covers the region 20° to 50°N, with three outcrop lines at $y_1 = 45.5$°N, $y_2 = 41$°N, and $y_3 = 35$°N. The first layer thickness along the eastern boundary is set to 300 m, and so the complete solution includes a shadow zone. We will carefully choose our forcing to limit its region of influence to the ventilated zone for simplicity. The Ekman pumping rate [cm s^{-1}] is $w_e = 1.0 \times 10^{-4} \sin\{[(y - y_s)/\Delta y]\pi\}$, where $y_s = 20$° and $\Delta y = 30$°.

The discussion presented here is for the case with cooling imposed on f_1; cooling/heating imposed on other outcrop lines can be treated in a similar way. A cooling anomaly is imposed in terms of a southward migration of the outcrop line with a small patch

$$\delta y_1 = \begin{cases} dy_1\left[1 - \left(\frac{x - x_0}{\Delta x}\right)^2\right]^{1/2}, \\ \quad \text{if } x_0 - \Delta x \le x \le x_0 + \Delta x \\ 0, \quad \text{otherwise}, \end{cases} \qquad (43)$$

where $x_0 = 20$°. We chose a small perturbation to illustrate the fundamental structure of the variability induced by a point source of buoyancy forcing, so $dy_1 = -0.01$° and $\Delta x = 4$° for the first experiment. Such an equatorial shift of the outcrop line represents a localized increase of the surface density due either to cooling of the surface or the production of a localized enhanced patch of salinity. The precise relation between such changes in surface temperature or salinity and the anom-

alous heat flux or precipitation/evaporation anomaly required to produce them is beyond the scope of our simple model. Since the perturbation solution is linear, the case of anomalous heating simply corresponds to a change of sign of all perturbation variables.

The climate variability is defined as the difference between the unperturbed solution and the perturbed solution. As discussed by Huang and Pedlosky (1999), surface cooling along f_1 leads to an increase of h_1 in the region of surface cooling. South of the first outcrop line, this primary potential vorticity anomaly propagates along ψ_1 and induces a decrease in h_2 in region II, as shown in the upper panels in Fig. 3. Thus, potential vorticity anomaly is created in layer 2.

Note that within these characteristic cones, the amplitude of the layer thickness perturbations varies over two orders of magnitude. In order to show the pattern of the perturbations over a large range a specially designed contour map is produced. First, the perturbation is converted into units of 0.1 mm. Second, all positive values are converted into $x = \log(dh)$, and all negative values of x are set to zero. Third, all negative values are converted into $x = -\log(-dh)$, and all positive values of x are set to zero. The horizontal pattern of the layer thickness perturbations is shown in Fig. 3. Even with just three outcrop lines, the pattern of the perturbations is rather complicated, and it is clear that the sign of layer thickness perturbations alternate in the horizontal plane.

South of f_2, the second layer is subducted, so the potential vorticity anomaly in the second layer is preserved and propagates along ψ_2. Thus, in region III we have two characteristic cones consisting of potential vorticity anomaly trajectories—the primary potential vorticity anomaly δq_1 that propagates along ψ_1 and the second potential vorticity anomaly δq_2 that propagates along ψ_2, as shown in Figs. 3a–c. Note that in the previous study by Huang and Pedlosky (1999) the discussion about a model with three moving layers is in error because the dynamic role of the secondary potential vorticity anomaly was overlooked.

South of f_3, the third layer is subducted, so the tertiary potential vorticity anomalies are created in the third layer, induced by the primary potential vorticity anomaly in the first layer and the secondary potential vorticity anomaly in the second layer. Thus, there are two new characteristics cones in region IV.

From the discussion above, we argue that the number of characteristic cones carrying the perturbation information doubles each time they cross a new outcrop line. The exponential growth of the number of characteristic cones is a major difficulty in dealing with the multilayer model. In this study we will focus on the case with four moving layers.

As the number of moving layer increases, the vertical structure of the perturbations becomes increasingly complicated. As shown in Eq. (5), variability induced by buoyancy forcing must appear in the form of internal
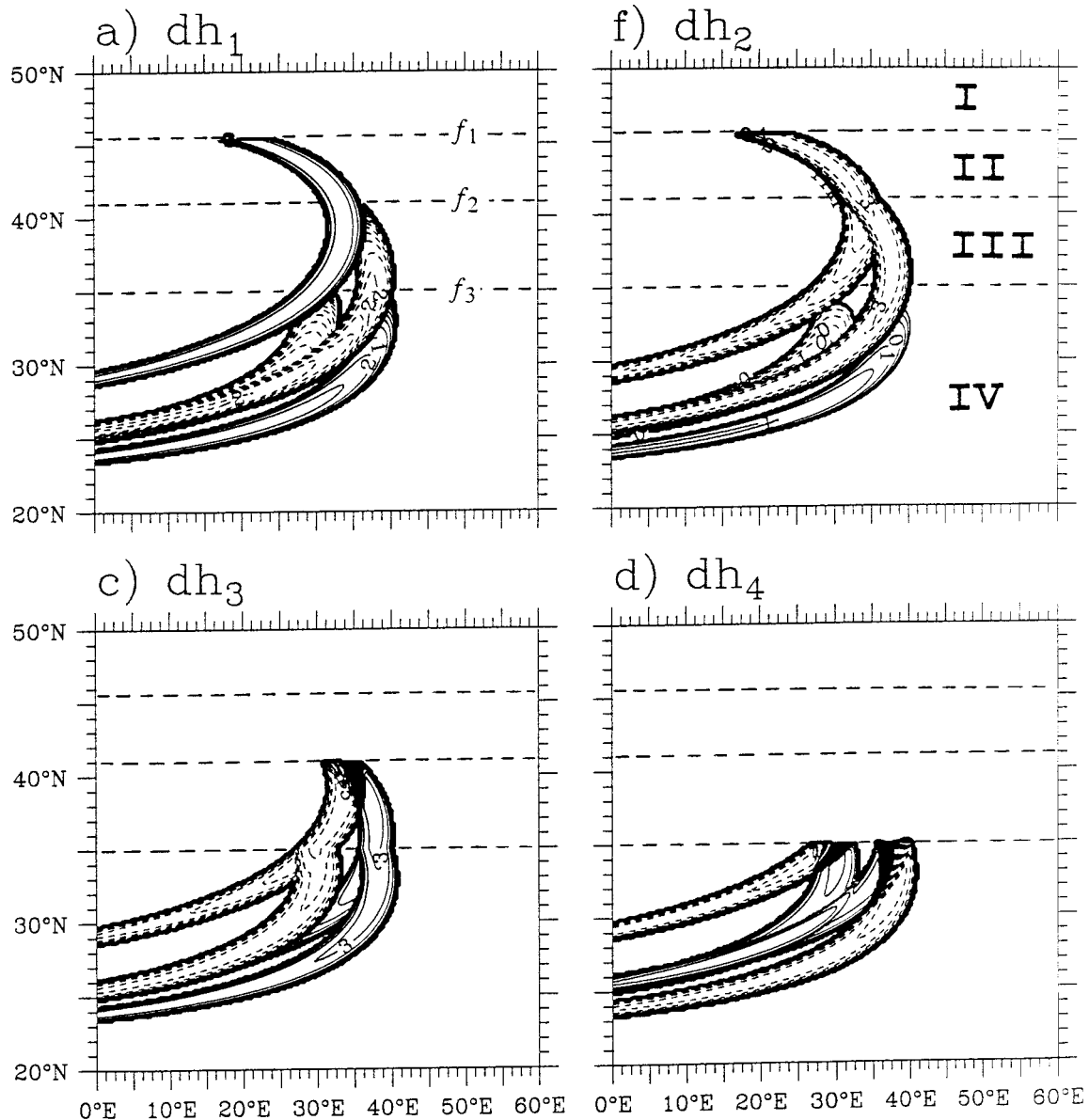
FIG. 3. Layer thickness perturbation maps, generated by cooling within a small area with $dy_1 = -0.01°$ and $\Delta x = 4°$. Three zonal dashed lines depict the outcrop lines, and I, II, III, and IV indicate different dynamic zones discussed in Fig. 2.

modes, the DTM. In region II, it appears in a second baroclinic DTM, M_2^1, where the subscript 2 indicates the number of moving layers and the superscript 1 indicates the layer where the driving potential vorticity source is located. The solution has been discussed by Huang and Pedlosky (1999).

In region III, the vertical structure of the solution in the two branches appears in different forms. Along the P branch (the primarily potential vorticity anomaly), the perturbation is in forms of M_3^1 mode. This mode is induced by a large positive dh_1. Along the S branch (the secondary potential vorticity anomaly), the perturbation is in the form of M_3^2 mode, which is induced by a neg-

ative dh_2 (Fig. 4). Note that $|dh_2| < |dh_1|$ because the former is secondary perturbation.

Note that within the S branch there are small potential vorticity (or layer thickness) perturbations in layer 1. Such perturbations are not directly related to the surface forcing on layer 1 at the outcrop line; instead, they are induced by the secondary potential vorticity anomaly in layer 2 in the following way. A potential vorticity anomaly in layer 2 induces a slight shift of streamlines in layer 1, and thus induces a change in the potential vorticity there. Similarly, there are small potential vorticity perturbations in layer 2 within branch P.
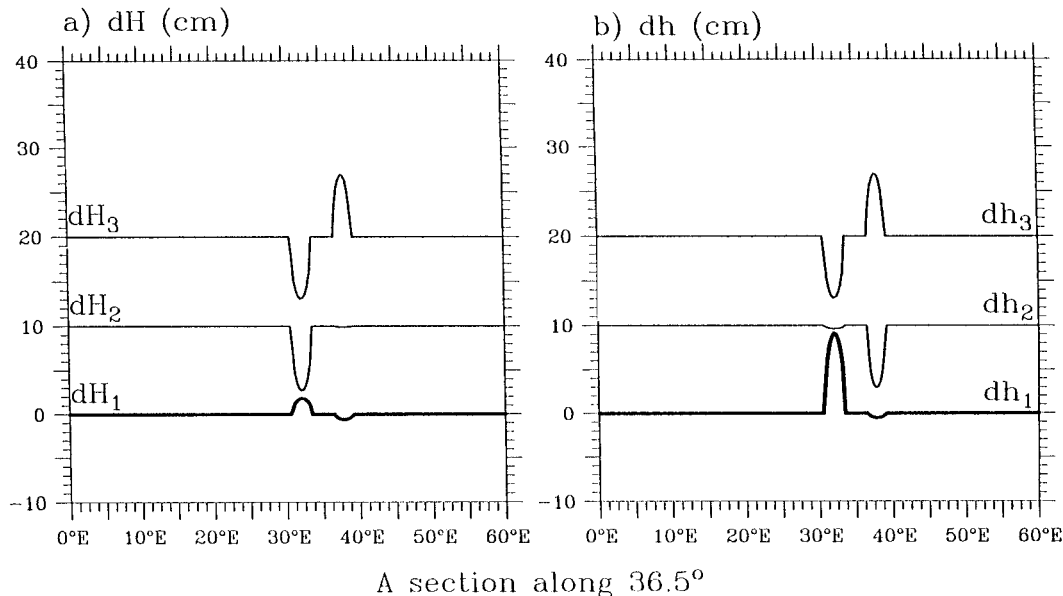
The vertical structure of the M_3^1 and M_3^2 are quite

FIG. 4. Perturbations of (a) interface depth and (b) layer thickness along 36.5°N, generated by cooling within a small area with $dy_1 = -0.01°$ and $\Delta x = 2°$. The curves for the second and third layer thickness (or interfacial depth) are shifted upward for a clear presentation.

different because they represent the thermocline's response to potential vorticity perturbations imposed on the first layer and the second layer respectively. In addition, we notice that the perturbation of the depth of the second interface has a very small negative value—due to the almost perfect compensation of the thickness perturbation of layers 2 and 3 (see Table 1).

In region IV, the vertical structure of the solution in the four branches are different, Fig. 5. The structure of the P branch is in forms of the M_4^1 mode, and the S branch is in forms of the M_4^2 mode. In comparison, the M_4^1 has a structure similar to the M_3^1, and the M_4^2 has a structure similar to the M_3^2.

There are two new characteristic cones, T_1 and T_2, that are generated by the tertiary potential vorticity in layer 3, induced by the primary (secondary) potential vorticity in layer 1 (2). The structure of these two branches is in forms of the M_4^3 mode, with opposite signs.

TABLE 1. Perturbations of interface depth ($dZ = -dH$) and layer thickness along 36.5°N (region III), in centimeters.

	Trajectory	
	P (dq_1)	S (dq_2)
	Location	
	32.1°E	37.8°E
dZ_3	6.90	−6.95
dZ_2	7.27	0.10
dZ_1	−1.81	0.59
dh_3	−6.90	6.95
dh_2	−0.37	−7.05
dh_1	9.08	−0.50

Since there are four moving layers, the vertical structure becomes more complicated, with the possibility of higher modes. However, we do not have a clear way of defining the higher modes in the DTM. Although, one can certainly define a set of eigenmodes and project the perturbation solution onto these eigenmodes, the meaning of such eigenmodes is not clear. The fundamental difficulty is that the perturbation solution to the thermocline equation involves not only the local stratification, but also other dynamic variables, such as the horizontal gradient of potential vorticity. Thus, any eigenfunction defined only by the local stratification does not carry the complete dynamic message implied by the thermocline structure of the unperturbed flow field.

Note that we have chosen a rather small amplitude perturbation of the outcrop line, $dy_1 = -0.01°$. For a realistic amplitude, say $dy_1 = -1°$, the perturbations shown in Tables 1 and 2 should increase 100 times.

Climate anomalies identified from climate records generally consist of a subsurface anomaly with a horizontal area large enough to survive for decades. As an example, we present a solution with $dy_1 = 0.5°$ and $\Delta x = 15°$, Fig. 6. Since the northward displacement corresponding to warming, the induced perturbations have opposite signs compared with the case of cooling. Furthermore, the anomaly has a finite amplitude, so all four branches overlap, leading to a complicated nonlinear solution within the characteristic cones. The interface depth and layer thickness perturbations are on the order of 5 m. The primary branch stands out clearly, while the secondary and tertiary branches merge. In this case we have chosen a small outcrop line displacement because for $\Delta x = 15°$ an outcrop line displacement larger
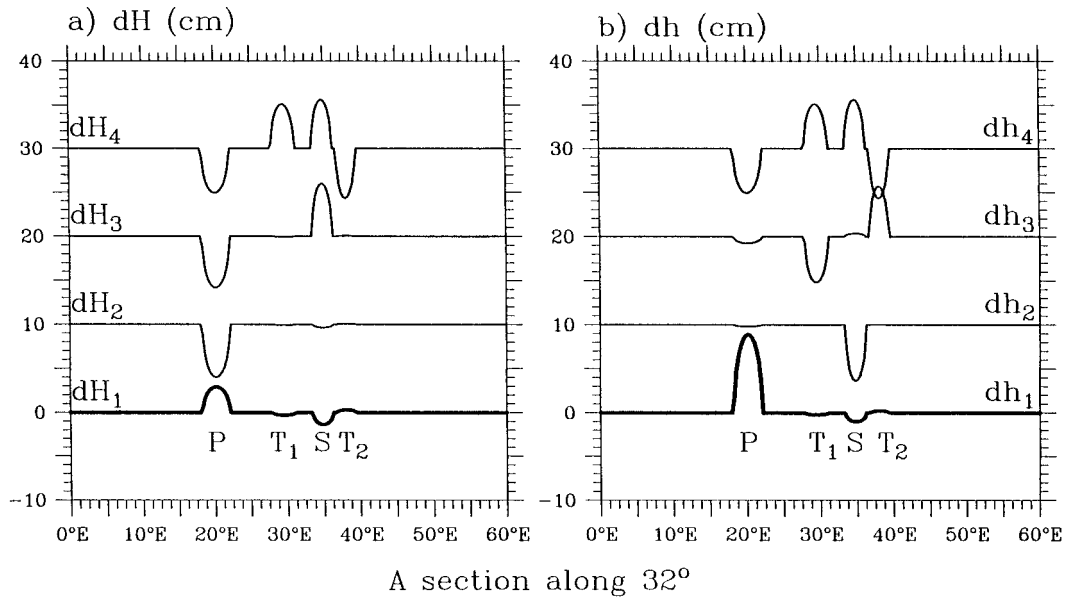
FIG. 5. Perturbations of (a) interface depth and (b) layer thickness along 32°N, generated by cooling within a small area with $dy_1 = -0.01°$ and $\Delta x = 2°$.

than 0.5° will lead to a nonmonotonic function $H_1(x)$ defined in (12). When $H_1(x)$ is nonmonotonic, one cannot invert this function to find the suitable outcrop line position. Physically, the nonmonotonic function $H_1(x)$ indicates that the slope of the outcrop line is too large, there is no consistent solution for the ventilated thermocline (e.g., Huang and Pedlosky 1999).

The structure of the perturbations on each isopycnal surface also look quite different compared with the previous cases. Now in the southern basin the four branches of the perturbations overlap, so there is no clearly defined boundary between them, Fig. 7. This is in contrast to the solution shown in Fig. 3, where each branch is well separated from the others. The overlapping of different branches of the perturbations may make the analysis of decadal climate variability more difficult.

Since the perturbation near the upper surface may be lost to influences from other anomalous forcing coming

into play later, only the subsurface perturbations will be likely to survive and can be identified from observations. From this four-layer model, we speculate that patterns shown in Fig. 6 may be a representative pattern for decadal climate variability in the oceans. Of course, this will either be confirmed or denied by further observations.

4. Discussion

As discussed by Huang and Pedlosky (1999), perturbations are horizontally confined within the characteristic cones defined by streamlines that carry the potential vorticity anomaly. The thickness of the lowest layer increases due to surface cooling, and the subduction of this layer creates the primary potential vorticity anomaly that drives the climate variability in the ventilated thermocline downstream.

Each time the characteristic cones carrying a potential vorticity anomaly cross a new outcrop line, the number of the characteristic cones involved in the perturbation doubles. In this paper, we present the climate variability of a four-moving-layer model of the ventilated thermocline. As the number of moving layers increases, the structure of the perturbation becomes exponentially complicated. The structure of perturbations to a model with a large number of moving layers is not clear at this time.

Suppose we double the number of layers used to represent the flow south of the outcrop line where the primary potential vorticity perturbation is created. Since the total density difference on the surface is invariant we must correspondingly halve the density differences between the new layers. As a consequence of the beta

TABLE 2. Perturbations of interface depth ($dZ = -dH$) and layer thickness along 32°N (region IV), in centimeters.

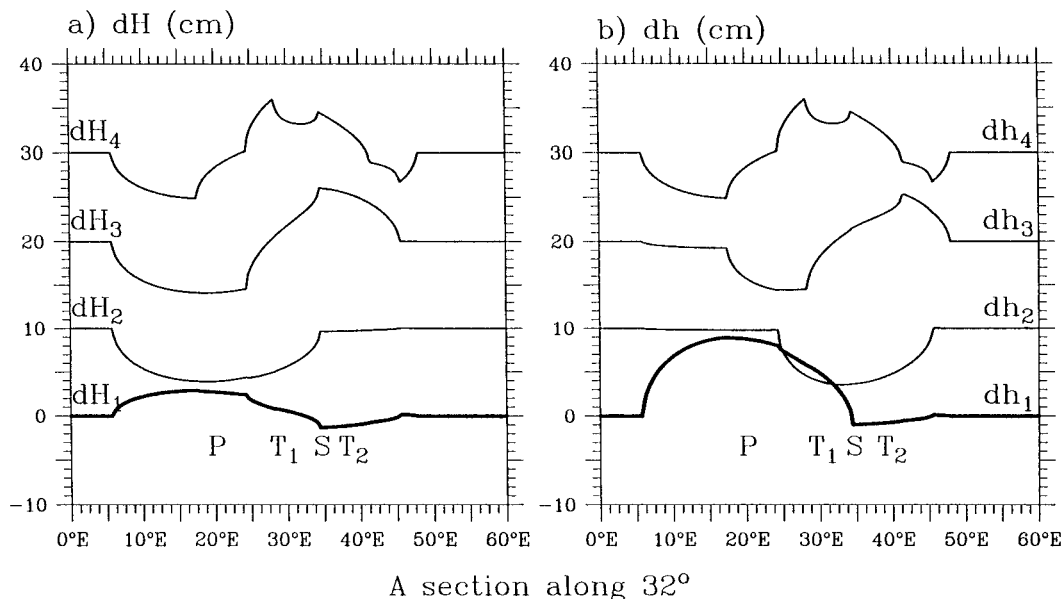|	Trajectory			
	P (dq_1)	T_1 (dq_{31})	S (dq_2)	T_2 (dq_{32})
	Location			
	20.1°E	29.4°E	34.8°E	38.1°E
dZ_4	5.08	−5.12	−5.65	5.67
dZ_3	5.82	0.05	−6.01	−0.06
dZ_2	6.00	0.07	0.35	−0.08
dZ_1	−2.92	0.29	1.35	−0.32
dh_4	−5.08	5.12	5.65	−5.67
dh_3	−0.74	−5.17	0.36	5.73
dh_2	−0.19	−0.02	−6.36	0.02
dh_1	8.92	−0.22	−1.01	0.24

FIG. 6. Pertubations of (a) interface depth and (b) layer thickness along 32°N, generated by heating within a large area with $dy_1 = 0.5°$ and $\Delta x = 15°$.

spiral (see, e.g., Pedlosky 1996) the turning angle between the flows in adjacent layers is proportional to the density difference between the layers and so would be correspondingly reduced as new layers are added. Hence we expect that in the limit of a continuously stratified fluid the eastern edge of the characteristic cone containing the anomalies would be grossly similar to our four-layer model. Although the streamlines in the most recently subducted layer always turn eastward, the overall pattern should tend to resemble the multilayer model although there may be a quantitative alteration in the limit. Note, though, that, as new layers are added, any eastward extension of the cone becomes thinner in the vertical direction. The numerical solutions with 20 ventilated layers provides some very interesting hints as to the structure of the climate variability, including complicated modal structure in both the horizontal and vertical directions (see Huang 2000).

However, we argue that, in principle, the overall domain of the perturbations is well defined, as shown in Fig. 8. First, the western edge of the perturbation (depicted by the solid line) is defined by the streamline in the layer where the primary potential vorticity is generated by surface cooling. Second, the eastern edge of the perturbation (depicted by the dashed line) is defined as an envelope in the following way. Starting from point P in Fig. 8, when the characteristic carrying the potential vorticity anomaly crosses a new outcrop line, a new characteristic carrying the potential vorticity anomaly induced in the layer above is created. Due to the rotation of the horizontal velocity, the so-called beta spiral, trajectories in the shallow layer travel to the right of the trajectories below. Thus, the streamline in the layer

above defines the eastern edge of the perturbation zone south of the new outcrop line.

Similarly, each time when the characteristics carrying the potential vorticity anomaly cross a new outcrop line, the signal is passed to the streamlines in the newly subducted layer above. Therefore, the envelope of the streamlines in the series of the most recently subducted layers defines the eastern edge of the perturbation zone in the model ocean, as shown by the dashed line in Fig. 8.

Accordingly, a point source of buoyancy forcing anomaly creates perturbations that propagate downstream within a characteristic cone. A given surface cooling anomaly of finite size can be treated as a superposition of such point sources, although the superposition is nonlinear in nature. Consequently, the variability induced by surface cooling can propagate to a location much closer to the equator than implied by the streamline carrying the primary potential vorticity anomaly. Although the vertical structure of the perturbations along the western edge of this characteristic cone is clearly defined by the nature of the primary potential vorticity, we do not know a priori the structure over the other parts of the characteristic cone at this time. As our calculations indicate, the anomaly at a given location may consist of either a local heating or cooling perturbation.

The perturbations created in the extratropics can propagate to the equatorial region, and a model of this process with a two moving layer has been discussed by Huang and Pedlosky (2000). However, for a multilayer model, such communication really is rather complicated. Most importantly, this communication depends on the position of the characteristic cone, car-
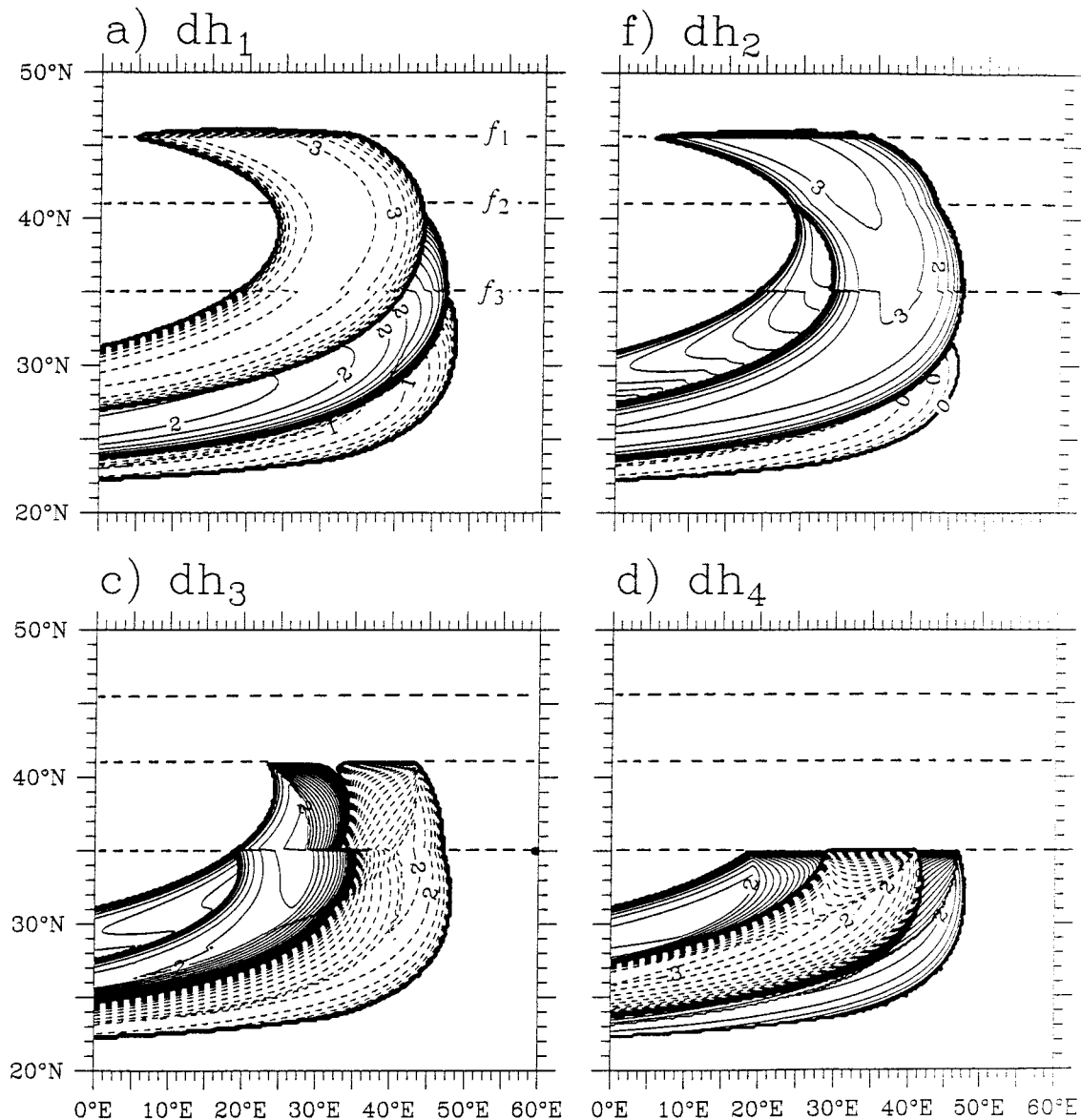
FIG. 7. Layer thickness perturbation maps, generated by heating within a large area with $dy_1 = 0.5°$ and $\Delta x = 15°$.
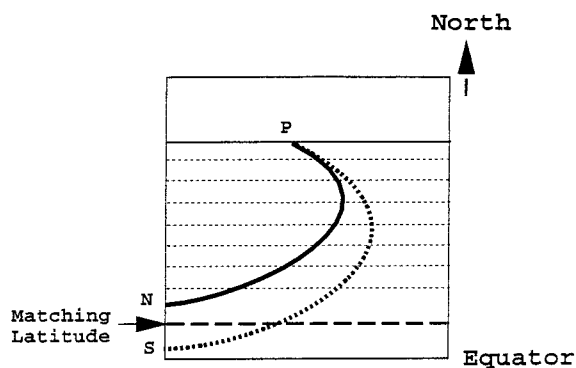
FIG. 8. A sketch illustrating the connection between midlatitude and equatorial athermocline.

rying the perturbations created in the extratropics, relative to the latitudinal location where the western boundary current bifurcates, as shown in Fig. 8.

If the southern edge of the characteristic cone (labled as S) is north of the matching latitude, all the perturbations should move northward, not affecting the equatorial thermocline. If the northern edge of the characteristic cone (labled as N) is south of the matching latitude, all perturbations should move into the equatorial thermocline. In particular, the primary potential vorticity anomaly should propagate to the equator. The climate variability at the equator induced by cooling at midlatitudes is discussed by Huang and Pedlosky (2000). On the other hand, if the characteristic cone straddles the matching latitude (as shown in Fig. 8),

only the southern part of the perturbation will move to the equatorial region, and its dynamic effect on the equatorial circulation is not clear because it depends on the structure of the perturbation within this part of the characteristic cone that remains a sensitive function of initial position.

APPENDIX

The Four-Layer Region

As discussed above, there are two sets of characteristics in region III, which carry the potential vorticity anomaly. If we imagine a point source of cooling along f_1, as these two characteristics across outcrop line f_3, each of them bifurcate, so there are four characteristics south of f_3; that is, a streamline in layer 1 (heavy solid line in Fig. 2) that carries the potential vorticity perturbation originally created in the cooling region, a streamline in layer 2 (heavy long-dashed line in Fig. 2) that carries a secondary potential vorticity anomaly created along f_2, and two streamlines in layer 3 that carry the tertiary potential vorticity anomaly, which is created when the first and second potential vorticity anomaly lines across the third outcrop line.

For the interior of region IV, we have the fractional layer thickness:

1) The first layer. The fractional thickness for the first layer is

$$F_1^{IV} = \frac{f}{f_{1,11}}, \qquad (A1)$$

where $f_{1,11}$ indicates that the position of the first outcrop line used here is obtained by tracing backward along streamline ψ_1 in regions IV, III, and II, as shown in Fig. 2.

2) The second layer. In order to determine the potential vorticity function Q_2, we notice that this function is set at point D along f_2. Repeating the same argument as in the previous section, we obtain the functional relation

$$Q_2(H_1 + \gamma_{21} H_2)$$

$$= \frac{f}{h_2} = \frac{f_2}{(1 - f_2/f_{1,22})} \frac{1 + \gamma_{21}\left(1 - \dfrac{f}{f_{1,22}}\right)}{H_1 + \gamma_{21} H_2}. \qquad (A2)$$

There are two differences, compared with the expression in region III: First, the second interfacial depth here is H_2 because there is one more moving layer here; second, $f_{1,2}$ is replaced by $f_{1,22}$ because now the corresponding outcrop position f_1 should be obtained by tracing ψ_2 in both regions IV and III.

Since in region IV

$$H_1 + \gamma_{21} H_2 = H_1\left[1 + \gamma_{21}\left(1 - \frac{f}{f_{1,11}}\right)\right], \qquad (A3)$$

the corresponding fractional layer thickness is

$$F_2^{IV} = \frac{f}{f_2}\left(1 - \frac{f_2}{f_{1,22}}\right)\frac{1 + \gamma_{21}\left(1 - \dfrac{f}{f_{1,11}}\right)}{1 + \gamma_{21}\left(1 - \dfrac{f}{f_{1,22}}\right)}. \qquad (A4)$$

3) The third layer. The potential vorticity in layer three is set up at point E along f_3 (Fig. 2). Along f_3, the fractional thickness for the first layer is

$$F_1^{IV} = \frac{f_3}{f_{1,31}}, \qquad (A5)$$

where $f_{1,31}$ indicates that the position of the first outcrop line is obtained by tracing back along ψ_3 in region IV, and then ψ_1 in region III.

On the other hand, the potential vorticity function Q_2 at this point is set up at point F along f_2 (Fig. 2). By following a similar analysis, we have the functional form of Q_2

$$Q_2'(H_1 + \gamma_{21} H_2)$$

$$= \frac{f_2}{(1 - f_2/f_{1,32})} \frac{1 + \gamma_{21}\left(1 - \dfrac{f_2}{f_{1,32}}\right)}{H_1 + \gamma_{21} H_2}, \qquad (A6)$$

where $f_{1,32}$ indicates that the position of the first outcrop line is obtained by tracing back along ψ_3 in region IV, and then ψ_2 in region III.

Approaching point E, f_1 is defined by $f_{1,31}$, that is, the position of the first outcrop line obtained by tracing backward along ψ_3 in region IV, and ψ_2 in region III. The corresponding fractional layer thickness is

$$(F_2^{IV})' = \frac{f}{f_2}\left(1 - \frac{f_2}{f_{1,32}}\right)\frac{1 + \gamma_{21}\left(1 - \dfrac{f}{f_{1,31}}\right)}{1 + \gamma_{21}\left(1 - \dfrac{f_2}{f_{1,32}}\right)}. \qquad (A7)$$

Along f_3, the fractional layer thickness for the lowest two moving layers are

$$F_{1,3}^{IV} = \frac{f_3}{f_{1,31}} \tag{A8}$$

$$F_{2,3}^{IV} = \frac{f_3}{f_2}\left(1 - \frac{f_2}{f_{1,32}}\right)\frac{1 + \gamma_{21}\left(1 - \dfrac{f_3}{f_{1,31}}\right)}{1 + \gamma_{21}\left(1 - \dfrac{f_2}{f_{1,32}}\right)}. \tag{A9}$$

Note that along f_3,

$$H_1 + \gamma_{21}H_2 + \gamma_{31}H_3$$
$$= H_1[1 + \gamma_{21}(1 - F_{1,3}^{IV})$$
$$+ \gamma_{31}(1 - F_{1,3}^{IV} - F_{2,3}^{IV})]. \tag{A10}$$

Thus, the potential vorticity function of layer 3 in region IV is

$$Q_3(x) = \frac{f_3}{1 - F_{1,3}^{IV} - F_{2,3}^{IV}}\frac{1}{H_1}$$

$$= \frac{f_3}{1 - F_{1,3}^{IV} - F_{2,3}^{IV}}$$
$$\times \frac{1 + \gamma_{21}(1 - F_{1,3}^{IV}) + \gamma_{31}(1 - F_{1,3}^{IV} - F_{2,3}^{IV})}{x}. \tag{A11}$$

Note that south of f_3,

$$H_1 + \gamma_{21}H_2 + \gamma_{31}H_3$$
$$= H_1[1 + \gamma_{21}(1 - F_1^{IV}) + \gamma_{31}(1 - F_1 - F_2^{IV})]. \tag{A12}$$

From these equations, we obtain the fractional layer thickness

$$F_1^{IV} = \frac{f}{f_{1,11}} \tag{A13}$$

$$F_2^{IV} = \frac{f}{f_2}\left(1 - \frac{f_2}{f_{1,22}}\right)\frac{1 + \gamma_{21}\left(1 - \dfrac{f}{f_{1,11}}\right)}{1 + \gamma_{21}\left(1 - \dfrac{f_2}{f_{1,22}}\right)} \tag{A14}$$

$$F_3^{IV} = \frac{f}{f_3}(1 - F_{1,3}^{IV} - F_{2,3}^{IV})$$
$$\times \frac{1 + \gamma_{21}(1 - F_1^{IV}) + \gamma_{31}(1 - F_1^{IV} - F_2^{IV})}{1 + \gamma_{21}(1 - F_{1,3}^{IV}) + \gamma_{31}(1 - F_{1,3}^{IV} - F_{2,3}^{IV})} \tag{A15}$$

$$F_4^{IV} = 1 - F_1^{IV} - F_2^{IV} - F_3^{IV}. \tag{A16}$$

4) How to determine the outcrop position. The calculation of the perturbed solution requires us to link the total depth of the ventilated thermocline H_1 at a given location to the corresponding total depth of the ventilated thermocline along f_1, $H_{1,0}$. For a given point in region IV there are five possible trajectories:

a) Determining $f_{1,11}$ by tracing backward along ψ_1: Since H_1 is conserved,

$$H_{1,0} = H_1. \tag{A17}$$

b) Determining $f_{1,21}$ by tracing backward along $\psi_2 \rightarrow \psi_1$: Since the streamlines ψ_2 are defined by $H_1 + \gamma_{21}H_2$,

$$H_1 + \gamma_{21}(H_1 - h_1)$$
$$= H_1\left[1 + \gamma_{21}\left(1 - \frac{f}{f_{1,11}}\right)\right]$$
$$= H_{1,0}\left[1 + \gamma_{21}\left(1 - \frac{f_3}{f_{1,21}}\right)\right]. \tag{A18}$$

Note that $f_{1,11}$ is the outcrop position for interior point, but $f_{1,21}$ is the corresponding outcrop position for the streamline that meets f_3. As a result, the relation for the total depth is

$$H_{1,0} = \frac{1 + \gamma_{21}\left(1 - \dfrac{f}{f_{1,11}}\right)}{1 + \gamma_{21}\left(1 - \dfrac{f_3}{f_{1,21}}\right)}H_1. \tag{A19}$$

c) Determining $f_{1,22}$ by tracing backward along $\psi_2 \rightarrow \psi_2$: Similar to the previous case, streamlines ψ_2 are defined by $H_1 + \gamma_{21}H_2$, so at f_3 the equivalent total depth is

$$H'_{1,0} = \frac{1 + \gamma_{21}\left(1 - \dfrac{f}{f_{1,11}}\right)}{1 + \gamma_{21}\left(1 - \dfrac{f_3}{f_{1,21}}\right)}H_1. \tag{A20}$$

From f_3 the trajectory is continued along ψ_2 northward; thus, a similar relation holds,

$$H_{1,0} = \frac{1 + \gamma_{21}\left(1 - \dfrac{f_3}{f_{1,21}}\right)}{1 + \gamma_{21}\left(1 - \dfrac{f_3}{f_{1,22}}\right)}H'_{1,0}$$

$$= \frac{1 + \gamma_{21}\left(1 - \dfrac{f}{f_{1,11}}\right)}{1 + \gamma_{21}\left(1 - \dfrac{f_2}{f_{1,22}}\right)}H_1. \tag{A21}$$

d) Determining $f_{1,31}$ by tracing backward along $\psi_3 \rightarrow \psi_1$: Streamlines ψ_3 is defined by $H_1 + \gamma_{21}H_2 + \gamma_{31}H_3$, so

$$H_1\left[1 + \gamma_{21}\left(1 - \frac{f}{f_{1,11}}\right) + \gamma_{31}\left(1 - \frac{f}{f_{1,11}} - F_2^{IV}\right)\right]$$

$$= H_{1,0}\left[1 + \gamma_{21}\left(1 - \frac{f_3}{f_{1,31}}\right)\right.$$

$$\left. + \gamma_{31}\left(1 - \frac{f_3}{f_{1,31}} - F_{2,3}^{IV}\right)\right].$$

Thus, along the $\psi_3 \to \psi_1$ trajectory, the depth ratio is

$$H_{1,0} = \frac{1 + \gamma_{21}\left(1 - \frac{f}{f_{1,11}}\right) + \gamma_{31}\left(1 - \frac{f}{f_{1,11}} - F_2^{IV}\right)}{1 + \gamma_{21}\left(1 - \frac{f_3}{f_{1,31}}\right) + \gamma_{31}\left(1 - \frac{f_3}{f_{1,31}} - F_{2,3}^{IV}\right)}H_1.$$

(A22)

e) Determining $f_{1,32}$ by tracing backward along $\psi_3 \to \psi_2$: There is a additional factor due to the contribution from the ψ_2 trajectory,

$$H_{1,0}'\left[1 + \gamma_{21}\left(1 - \frac{f_3}{f_{1,31}}\right)\right]$$

$$= H_{1,0}\left[1 + \gamma_{21}\left(1 - \frac{f_2}{f_{1,32}}\right)\right].$$ (A23)

Therefore, the depth ratio is

$$H_{1,0} = \frac{1 + \gamma_{21}\left(1 - \frac{f}{f_{1,11}}\right) + \gamma_{31}\left(1 - \frac{f}{f_{1,11}} - F_2^{IV}\right)}{1 + \gamma_{21}\left(1 - \frac{f_3}{f_{1,31}}\right) + \gamma_{31}\left(1 - \frac{f_3}{f_{1,31}} - F_{2,3}^{IV}\right)}$$

$$\times \frac{1 + \gamma_{21}\left(1 - \frac{f_3}{f_{1,31}}\right)}{1 + \gamma_{21}\left(1 - \frac{f_2}{f_{1,31}}\right)}H_1.$$ (A24)

REFERENCES

Huang, R. X., 2000: Climate variability inferred from a continuously stratified model of the ideal-fluid thermocline. *J. Phys. Oceanor.,* **30,** 1389–1406.

——, and J. Pedlosky, 1999: Climate variability inferred from a layered model of the ventilated thermocline. *J. Phys. Oceanogr.,* **29,** 779–790.

——, and ——, 2000: Climate variability of the equatorial thermocline inferred from a two-moving-layer model of the ventilated thermocline. *J. Phys. Oceanogr.,* **30,** 2610–2626.

Luyten, J. R., J. Pedlosky, and H. Stommel, 1983: The ventilated thermocline. *J. Phys. Oceanogr.,* **13,** 292–309.

Pedlosky, J., 1996: *Ocean Circulation Theory.* Springer-Verlag, 453 pp.

United States Postal Service

Statement of Ownership, Management, and Circulation

1. Publication Title	2. Publication Number								3. Filing Date
Journal of Physical Oceanography	0	0	2	2		3	6	7	0	October 1, 2000

4. Issue Frequency	5. Number of Issues Published Annually	6. Annual Subscription Price
Monthly	12	$55.00 Members $420.00 Non Members

7. Complete Mailing Address of Known Office of Publication *(Not printer) (Street, city, county, state, and ZIP+4)*	Contact Person Mary McMahon
45 Beacon Street, Boston, Suffolk, Mass. 02108-3693	Telephone 617-227-2426 x 218

8. Complete Mailing Address of Headquarters or General Business Office of Publisher *(Not printer)*

45 Beacon Street, Boston, Mass. 02108-3693

9. Full Names and Complete Mailing Addresses of Publisher, Editor, and Managing Editor *(Do not leave blank)*

Publisher *(Name and complete mailing address)*

American Meteorological Society, 45 Beacon Street, Boston, Mass. 02108-3693

Editor *(Name and complete mailing address)*

Dr. Peter Muller, School of Ocean, Earth Science & Technology
University of Hawaii, 1000 Pope Rd, MSB 429
Honolulu, Hawaii 96822

Managing Editor *(Name and complete mailing address)*

Dr. Ronald D. McPherson, American Meteorological Society
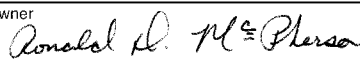45 Beacon Street, Boston, Mass. 02108-3693

10. Owner *(Do not leave blank. If the publication is owned by a corporation, give the name and address of the corporation immediately followed by the names and addresses of all stockholders owning or holding 1 percent or more of the total amount of stock. If not owned by a corporation, give the names and addresses of the individual owners. If owned by a partnership or other unincorporated firm, give its name and address as well as those of each individual owner. If the publication is published by a nonprofit organization, give its name and address.)*

Full Name	Complete Mailing Address
American Meteorological Society	45 Beacon Street, Boston, Mass. 02108-3693

11. Known Bondholders, Mortgagees, and Other Security Holders Owning or Holding 1 Percent or More of Total Amount of Bonds, Mortgages, or Other Securities. If none, check box ────────────▶ ☑ None

Full Name	Complete Mailing Address

12. Tax Status *(For completion by nonprofit organizations authorized to mail at nonprofit rates) (Check one)*

The purpose, function, and nonprofit status of this organization and the exempt status for federal income tax purposes:

☑ Has Not Changed During Preceding 12 Months

☐ Has Changed During Preceding 12 Months *(Publisher must submit explanation of change with this statement)*

PS Form **3526,** September 1998   *(See Instructions on Reverse)*

13. Publication Title Journal of Physical Oceanography			14. Issue Date for Circulation Data Below June 2000	

15. Extent and Nature of Circulation			Average No. Copies Each Issue During Preceding 12 Months	No. Copies of Single Issue Published Nearest to Filing Date
a. Total Number of Copies *(Net press run)*			1536	1450
b. Paid and/or Requested Circulation	(1)	Paid/Requested Outside-County Mail Subscriptions Stated on Form 3541. *(Include advertiser's proof and exchange copies)*	1076	1057
	(2)	Paid In-County Subscriptions *(Include advertiser's proof and exchange copies)*	0	0
	(3)	Sales Through Dealers and Carriers, Street Vendors, Counter Sales, and Other Non-USPS Paid Distribution	0	0
	(4)	Other Classes Mailed Through the USPS	0	0
c. Total Paid and/or Requested Circulation *[Sum of 15b. (1), (2),(3),and (4)]* ▶			1076	1057
d. Free Distribution by Mail *(Samples, complimentary, and other free)*	(1)	Outside-County as Stated on Form 3541	0	0
	(2)	In-County as Stated on Form 3541	0	0
	(3)	Other Classes Mailed Through the USPS	0	0
e. Free Distribution Outside the Mail *(Carriers or other means)*			20	20
f. Total Free Distribution *(Sum of 15d. and 15e.)* ▶			20	20
g. Total Distribution *(Sum of 15c. and 15f)* ▶			1096	1077
h. Copies not Distributed			440	373
i. Total *(Sum of 15g. and h.)* ▶			1536	1450
j. Percent Paid and/or Requested Circulation *(15c. divided by 15g. times 100)*			98.2%	98.1%

16. Publication of Statement of Ownership   November 2000
☑ Publication required. Will be printed in the _____ issue of this publication.   ☐ Publication not required.

17. Signature and Title of Editor, Publisher, Business Manager, or Owner

Dr. Ronald D. McPherson, Executive Director   *Ronald D. McPherson*   Date July 24, 2000

I certify that all information furnished on this form is true and complete. I understand that anyone who furnishes false or misleading information on this form or who omits material or information requested on the form may be subject to criminal sanctions (including fines and imprisonment) and/or civil sanctions (including civil penalties).

Instructions to Publishers

1. Complete and file one copy of this form with your postmaster annually on or before October 1. Keep a copy of the completed form for your records.

2. In cases where the stockholder or security holder is a trustee, include in items 10 and 11 the name of the person or corporation for whom the trustee is acting. Also include the names and addresses of individuals who are stockholders who own or hold 1 percent or more of the total amount of bonds, mortgages, or other securities of the publishing corporation. In item 11, if none, check the box. Use blank sheets if more space is required.

3. Be sure to furnish all circulation information called for in item 15. Free circulation must be shown in items 15d, e, and f.

4. Item 15h., Copies not Distributed, must include (1) newsstand copies originally stated on Form 3541, and returned to the publisher, (2) estimated returns from news agents, and (3), copies for office use, leftovers, spoiled, and all other copies not distributed.

5. If the publication had Periodicals authorization as a general or requester publication, this Statement of Ownership, Management, and Circulation must be published; it must be printed in any issue in October or, if the publication is not published during October, the first issue printed after October.

6. In item 16, indicate the date of the issue in which this Statement of Ownership will be published.

7. Item 17 must be signed.

Failure to file or publish a statement of ownership may lead to suspension of Periodocals authorization.

PS Form **3526**, September 1998 *(Reverse)*